Interaction of soil water and groundwater during the freezing-thawing cycle: field observations and numerical modeling

5   Hong-Yu Xie[1], Xiao-Wei Jiang[1*], Shu-Cong Tan[1], Li Wan[1], Xu-Sheng Wang[1], Yijian Zeng[2]

1. MOE (Ministry of Education) Key Laboratory of Groundwater Circulation and Evolution, China University of Geosciences, Beijing 100083, China

2. Department of Water Resources, ITC Faculty of Geo-Information Science and Earth Observation, University of Twente, Enschede, the Netherlands

10   *Correspondence to: Xiao-Wei Jiang (jxw@cugb.edu.cn)

Abstract

Freezing-induced water migration and groundwater level decline are widely observed in regions with shallow water table, but many existing studies trying to quantify freezing-induced groundwater migration do not account for water level fluctuations induced by freezing and thawing. Here, detailed field observations of liquid soil water content and groundwater level fluctuations at a site in the Ordos Plateau, China are combined with numerical modeling to show groundwater and soil water dynamics controlled by wintertime atmospheric conditions and topographically-driven lateral groundwater inflow. By comparing simulation results with and without lateral groundwater inflow, we find lateral groundwater inflow leads to an alleviated freezing-induced water level decline and enhanced freezing-induced water migration. At the field site with a lateral groundwater inflow rate of 1.03 mm/d, compared with the case without lateral groundwater inflow, the water level decline decreases from 40 cm to 15 cm, and the increased total water content in the frozen zone enhances from 0.071 to 0.106. By calculating the budget of groundwater, the mean upward flux of freezing-induced groundwater loss is 1.46 mm/d for 93 days, and the mean flux of thawing-induced groundwater gain is as high as 3.94 mm/d for 32 days. The study enhances our understanding of the mechanisms controlling water redistribution between saturated and unsaturated zones and the water budget in the freezing-thawing cycle. The fluxes of groundwater loss and gain in the freezing and thawing stages obtained in the current study can be useful for future studies on two- or three-dimensional transient groundwater flow in semi-arid regions with seasonally frozen soils.

1 Introduction

30   Frozen soils have great impacts on many hydrological, hydrogeological processes and ecological processes (Nelson, 2003;Kurylyk et al., 2014;Schuur et al., 2015;Walvoord and Kurylyk, 2016;Evans et al., 2018;Zhang et al., 2020). In fact, frozen soils can be divided into permafrost and seasonally frozen soils, which underlie approximately 26% and 24%, respectively, of the Northern Hemisphere exposed land surface (Zhang et al., 2003;Dobinski, 2011;Evans and Ge, 2017). The behaviors of subsurface water flow and storage in seasonally

35   frozen soils are distinct from both colder regions with permafrost and warmer regions with insignificant frozen soil (Ireson et al., 2013). Understanding the effects of soil freezing and thawing on subsurface water flow and storage is a necessary path for better water resources management in (semi-)arid regions with occurrence of seasonally frozen soils (Yu et al., 2020).

     In seasonally frozen regions, by blocking pores and reducing hydraulic conductivity, soil freezing could lead

40   to decreased infiltration (van der Kamp et al., 2003;Iwata et al., 2008;Demand et al., 2019) and limited surface evaporation (Kaneko et al., 2006;Wu et al., 2016). Soil freezing also generated cryosuction (Williams and Smith, 1989;Hohmann, 1997;Yu et al., 2018), which causes migration of water from the unfrozen zone to the freezing front and further decrease the hydraulic conductivity of frozen soils. By assuming that freezing-induced water migration is restricted within the shallow part of unsaturated zone which is far away from the water table, many

45   numerical studies deployed a free drainage lower boundary condition and examined the effects of freezing-induced water redistribution on infiltration and runoff (Cherkauer and Lettenmaier, 1999;Okkonen et al., 2017;Zhang et al., 2017). In fact, freezing-induced water movement is not restricted within the unsaturated zone, and water could be migrated from the saturated zone through the unsaturated zone to the freezing front (Harlan, 1973;van der Kamp, 1992;Ireson et al., 2013). Since the 1950s, there are many field observations of

50   freezing-induced groundwater level decline (Drescher, 1955;Schneider, 1961;Stähli et al., 1999;Daniel and Staricka, 2000;van der Kamp et al., 2003;Ireson et al., 2013;Zhang et al., 2019), which are closely related to shallow groundwater in topographic lows (Gleeson et al., 2011;Fan et al., 2013). Unfortunately, numerical research on freezing-induced water redistribution that satisfactorily considers freezing-induced groundwater level decline is limited, which restricts quantitative understanding of water budgets in the freezing/thawing cycle.

55   To understand the effects of soil freezing on hydrogeological and ecohydrological processes and engineering problems, a key knowledge is the amount of freezing-induced water migration from the saturated zone to the frozen zone. Freezing-induced water migration from the saturated zone to the freezing front would

necessarily strengthen the possibility of frost heave (Chamberlain, 1981;Bronfenbrener and Bronfenbrener, 2010;Rui et al., 2019). During the thawing stage, accumulation of thawed water above the frozen zone would

60   accelerate soil evaporation (Fetzer et al., 2017;Vanderborgh et al., 2017;Li et al., 2020), which is critical to soil salinization (Liu et al., 2009;Lopez et al., 2010;Bechtold et al., 2011). In some previous experimental and numerical studies, freezing-induced water migration from groundwater to the frozen zone was obtained by assuming a fixed water table (Shoop and Bigl, 1997;Hansson and Lundin, 2006;Alkhaier et al., 2012;Chen et al., 2019). In fact, a fixed water table lower boundary condition is an over-simplified representation of groundwater

65   conditions (Carrera-Hernández et al., 2012), which implies that loss of groundwater can be replenished instantaneously. It has been found that a fixed water table would overestimate evaporation-induced groundwater loss (Zhu et al., 2010;Zhao et al., 2020). However, the degree of overestimation of freezing-induced groundwater migration by using a fixed head lower boundary condition remains unknown.

As initially proposed by Hubert (1940) and Tóth (1962), lateral groundwater flow is ubiquitous in regions

70   with undulating topography and water table. Although wintertime water table fluctuations caused by freezing and thawing have been widely recognized (Willis et al., 1964;van der Kamp et al., 2003;Zhang et al., 2019), the simultaneous contribution of lateral groundwater flow to wintertime water table fluctuations received little attention. Ireson et al. (2013) found the wintertime water table recessions in their two study sites in the Canadian prairies were partly due to lateral groundwater outflow, while Jiang et al. (2017) found the pattern of wintertime

75   water table fall-rise in their study site in the Ordos Plateau, China was also influenced by lateral groundwater inflow. Therefore, the wintertime water table dynamics is not prior known, but is a function of both atmospheric conditions and lateral groundwater inflow/outflow and should be a part of model output. To obtain a clear understanding of wintertime water migration in regions with shallow groundwater, it is appealing to numerically combine hydrological processes in both saturated and unsaturated zones, including topographically-driven lateral

80   flow in the saturated zone, freezing-induced water migration from the saturated to the unsaturated zone, and thawing-induced water movement. In the current study, the field site reported in Jiang et al. (2017), which has shallow water table and lateral groundwater inflow, is used to numerically examine the interactions of soil water and groundwater and calculate the water budget during the freezing-thawing cycle.

2 Methods

85   ### 2.1 Study area and conceptual model

The Ordos Plateau in Northwestern China is one of the most intensively studied groundwater basins due to its

dependence on groundwater (Hou et al., 2010;Jiang et al., 2018). The main aquifer is the thick Cretaceous sandstone, which is overlain by thin Quaternary sediments. Due to the spatially undulating topography and low permeability of the sandstone aquifer, water table undulation is a subdued replica of the topography and regional

90   groundwater generally flows laterally from topographic highs to topographic lows of a catchment. In a specific catchment, as a result of the occurrence of a small lake in topographic lows and the contribution of lateral groundwater flow from topographic highs, water table is shallow in topographic lows near the lake.

The Ordos Plateau has a semi-arid and cold climate. According to the meteorological data in the Otak station from 1955 to 2016 (data from China Meteorological Data Service Center, available at http://data.cma.cn),

95   the annual mean precipitation is 265 mm and the annual mean evaporation is 1370 mm. The average monthly temperature decreases from -1.5 ℃ in November to -10.4 ℃ in January and increases from -6.4 ℃ in February to 0.9 ℃ in March, therefore, the period from late November to late March corresponds to the freezing-thawing cycle. Groundwater level declines induced by evapotranspiration in the summer and by freezing in the winter have been reported in some sites with shallow groundwater (Jiang et al., 2017;Zhang et al., 2019). The

100   relationship between groundwater, soil water and the summertime atmospheric conditions, i.e., infiltration and evapotranspiration, has been numerically coupled by some researchers (Chen et al., 2019;Zhao et al., 2020). However, there is no numerical study on how groundwater and soil water dynamics respond to wintertime atmospheric conditions.

The Wudu Lake catchment is one of the small catchments located to the southeast of the first-order water

105   divide of the Ordos Plateau. The distribution of water table elevations in the Wudu lake catchment can be found in Jiang et al. (2018) while the zone of flowing wells, i.e., with higher hydraulic head than the topography, can be found in Wang et al. (2015). There is a monitoring site of soil water content and groundwater level in the topographic lows of this catchment. The occurrence of several flowing wells near the monitoring site indicates that the site belong to the discharge area and could receive lateral groundwater flow from topographic highs. The

110   water table depths are recorded by using water level loggers in a shallow well with a depth of 10 m while the temperatures and liquid water content in the Quaternary deposits are recorded by using 5TM sensors produced by Decagon Devices at 8 depths (at around 10 cm, 20 cm, 30 cm, 50 cm, 70 cm, 90 cm, 110 cm, 150 cm). As shown in Fig. 1, water table depth increases from 115 cm on 28 NOV 2015 to 143 cm on 29 JAN 2016, which is a direct result of freezing-induced water migration from groundwater to the freezing front.

115   At the monitoring site, lateral groundwater flow had been found to be an indispensable component of groundwater budget (Jiang et al., 2017). Fig. 2 shows the control of main hydrological and hydrogeological

processes on groundwater level during the freezing-thawing cycle. The processes leading to water level decline

include water migration induced by freezing and evaporation due to the dry climate, and the processes leading to

water level rise is lateral groundwater flow throughout the cycle and infiltration of thawed water during the

120   thawing stage.
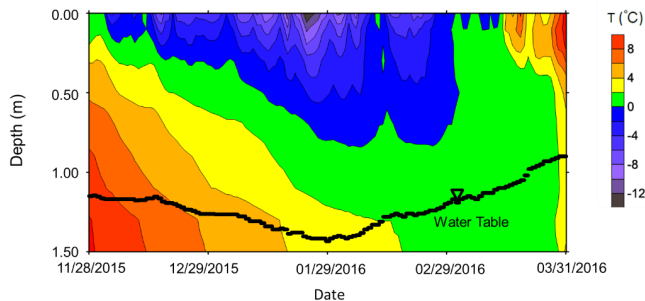
Figure 1. The contour map showing the change of soil temperature at the study site during the freezing-thawing

cycle. Also shown is the fluctuating groundwater level monitored at the study site.
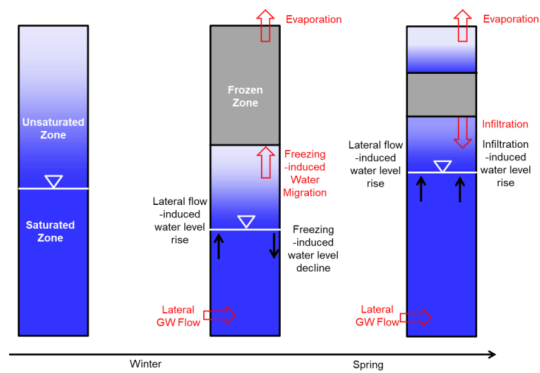
125   Figure 2 The conceptual models of hydrological processes and groundwater regime in semi-arid regions during

the seasonally freezing and thawing stages.

2.2. The SHAW model

The Simultaneous Heat and Water (SHAW) model (Flerchinger and Saxton, 1989) is one of the most robust

models for freezing-induced water migration (Hayhoe, 1994;DeGaetano et al., 2001;Kahimba et al., 2009;Zhang

130   et al., 2017). The contributions of liquid water, ice, and vapor contents have been considered in the water balance

equation, and the contributions of heat conduction, phase change, liquid flow, and vapor gas diffusion have been

considered in the energy balance equation (Li et al., 2010). Because water flow in the unsaturated zone is

predominantly vertical (Stephens, 1996;Romano et al., 1998;Van Dam and Feddes, 2000), the SHAW model only

accounts for the effects of soil freezing and thawing on water redistribution within a one-dimensional (1D) soil

135 column. Moreover, by adding a source term in the water balance equation, it has the ability to account for the

contribution of lateral groundwater flow to water level in the soil column. Therefore, the SHAW model is suitable

to couple the groundwater dynamics with soil water dynamics during the freezing-thawing cycle as observed in

our field site.

Considering convective heat transfer by liquid, latent heat transfer by ice and latent heat transfer by vapor,

140 the energy balance equation in the soil matrix is expressed as

$$C_s \frac{\partial T}{\partial t} - \rho_i L_f \frac{\partial \theta_i}{\partial t} = \frac{\partial}{\partial z}\left[k_T \frac{\partial T}{\partial z} \right] - \rho_l c_l \frac{\partial q_l T}{\partial z} - L_v \left[\frac{\partial q_v}{\partial z} + \frac{\partial \rho_v}{\partial t} \right] \tag{1}$$

where T is temperature [Θ], θ_i is volumetric ice content [-], z is soil depth [L], t is time [T], ρ_i, ρ_l and ρ_v are

densities of ice, liquid water and vapor [M L^{-3}], respectively, L_f and L_v are latent heat of fusion and vaporization

[L^2 T^{-2}], respectively, q_l is liquid water flux [L T^{-1}], q_v is water vapor flux [M L^{-2} T^{-1}], c_l is specific heat capacity of

145 water [L^2 T^{-2} Θ^{-1}], C_s is volumetric heat capacity of soil [M L^{-2} T^{-2} Θ^{-1}], and k_T is thermal conductivity of soil [M L^2

T^{-3} Θ^{-1}]. Calculation of C_s and k_T can be found in Flerchinger and Saxton (1989) and is not reproduced here.

By considering ice content change and vapor flux, the water balance equation is written as

$$\frac{\partial \theta_l}{\partial t} + \frac{\rho_i}{\rho_l} \frac{\partial \theta_i}{\partial t} = \frac{\partial}{\partial z}\left[K\left(\frac{\partial \psi}{\partial z} + 1 \right) \right] + \frac{1}{\rho_l} \frac{\partial q_v}{\partial z} + U \tag{2}$$

where θ_l is liquid water content [-], K is hydraulic conductivity [L T^{-1}], ψ is soil matric potential [L], and U is a

150 source/sink term for water flux [T^{-1}]. Soil water characteristic curves, which describe the relationship between soil

matric potential and liquid water content, are defined for both unfrozen and frozen soils. Here, the van Genuchten

equation (van Genuchten, 1980) is selected, which is written as

$$\frac{\theta_l - \theta_r}{\theta_s - \theta_r} = \left(1 + |\alpha\psi|^n \right)^{-m} \tag{3}$$

where θ_s and θ_r are saturated and residual water content [-], α [L^{-1}], n [-] and m [-] are empirical parameters. α

155 equals the inverse of the air-entry value, n is a pore-size distribution index and $m=1-1/n$. In the frozen zone, due to

the co-existence of liquid water and ice, matric potential is strongly dependent on temperature, and the matric

potential is obtained by the following equation (Fuchs et al., 1978):

$$\psi = \frac{L_f}{g} \frac{T}{T + 273.15} \tag{4}$$

where g is the acceleration of gravity [L T^{-2}]. Eq. (4) indicates that as the negative temperature increases, the soil

160 suction also increases (matric potential becomes more negative).

The hydraulic conductivity of the unfrozen zone is computed by

$$K = K_s S_e^l \left[1 - \left(1 - S_e^{1/m} \right)^m \right]^2 \tag{5}$$

where K_s is the saturated hydraulic conductivity [L T^{-1}], S_e [-] is the effective saturation calculated by

$(\theta_l - \theta_r)/(\theta_s - \theta_r)$, and l [-] is a pore-connectivity parameter which is assumed to be 0.5 in the original work of

165   (Mualem, 1976). Note that in the saturated unfrozen zone, K equals K_s, but in the unsaturated unfrozen zone,

K equals unsaturated hydraulic conductivity (K_u). In the frozen zone, due to occupation of ice in the pores,

the unsaturated hydraulic conductivity computed from Eq. (5) is reduced linearly with ice content and is

assumed to be zero when the porosity is decreased to 0.13 (Flerchinger, 2000).

2.3. Model inputs

170   In the following, based on the conceptual model shown in Figure 2, we use SHAW to couple soil water and

groundwater dynamics in a 1D soil column during the freezing-thawing cycle from 28 NOV 2015 to 1 APR 2016,

as such to understand how the coupled unsaturated-saturated processes respond to wintertime atmospheric

conditions. To ensure that the lateral groundwater inflow occurs within the saturated zone, the length of the 1D

soil column is set to be 155 cm. The model domain is uniformly divided into 31 layers, which results in 32 nodes.

175   The top node has an atmospheric boundary condition, while the bottom node has a zero-flux and

specified-temperature. Following Flerchinger (2000), the occurrence of lateral groundwater flow is realized by

setting a specified hydraulic gradient at the 31st node. The fluctuation of groundwater level is an outcome of

wintertime atmospheric conditions and lateral groundwater flow, while the fluctuations of soil water content are

controlled by both wintertime atmospheric conditions and groundwater dynamics.

180   The inputs for the atmospheric boundary condition include maximum air temperature, minimum air

temperature, wind speed, precipitation, solar radiation and dew-point temperature. The first four parameters

available from the observations at the Otak meteorological stations, the parameter of solar radiation is calculated

by the Angström-Prescott equation (Yorukoglu and Celik, 2006) based on the sunshine duration (data available

from China Meteorological Data Service Center), and the dew-point temperature is calculated by the

185   Hyland-Wexter equation (Wexler et al., 1983) based on relative humidity, maximum air temperature and

minimum air temperature. Fig. 3 shows the maximum and minimum air temperatures, dew-point temperature and

precipitation. The inputs for the lower boundary condition at the bottom include a zero hydraulic conductivity to

insure a no-flux boundary condition, and the daily averaged soil temperature measured at approximately

corresponding depth for the specified-temperature boundary condition. The model spin-up is run for 30 days

190   before the start of freezing time (28 NOV 2015) to reach a quasi-steady state. The initial conditions of soil water

content and soil temperature for spin-up are determined based on measured values on 29 OCT 2015.
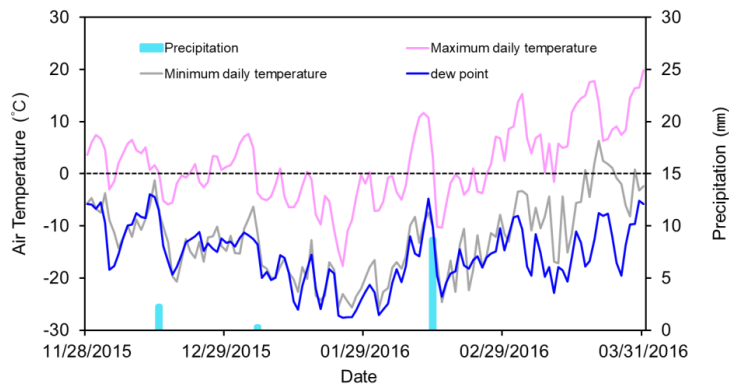
Figure 3 the maximum daily air temperature, the minimum air temperature, dew-point temperature and precipitation during the freezing-thawing cycle from 28 NOV 2015 to 1 APR 2016.

195

Although soil samples from all depths belong to sand or loamy sand, soil texture differs in the profile. The percentage of clay ranges between 5 and 8% in the layer between 70 and 100 cm, and between 1 and 4% in other depths (Zhao et al., 2020). Therefore, the model domain is divided into three layers. The parameters for the van Genuchten (1980) and Mualem (1976) models obtained by Zhao et al. (2020) are further calibrated, which are

200 shown in Table 1. As shown in Table 2, the further calibrated parameters result in much lower RMSEs. Based on the possible range of lateral flow rate varying between 0.96 and 1.16 mm/d (Jiang et al., 2017), the lateral inflow rate is calibrated to be 1.03 mm/d, which leads to the lowest RMSE of water table depth. This base case is denoted as Scenario A in Sect. 3.2.

To examine the role of soil heterogeneity in freezing-induced water migration, in Scenario B, we assume

205 the whole soil column has the same soil texture as that of 0 cm to 70 cm, and all other conditions are kept unchanged as Scenario A. By setting the lateral inflow rate to be zero, Scenario A changes into Scenario C and Scenario B changes into Scenario D. Because the disappearance of lateral groundwater inflow would lead to much deeper water table depth, the length of the 1D soil column in Scenarios C and D is extended to 200 cm. In Scenario C, the layer from 155 cm to 200 cm is assumed to have the same soil texture as that from 100 cm to 155

210 cm. Because there is no temperature measurement at 200 cm, the temperature at the lower boundary is estimated by the method proposed by Hirota (2002), which is based on heat conduction and energy balance.

Table 1 Calibrated hydraulic parameters for the van Genuchten (1980) and Mualem (1976) models

Depth (m)	θ_r (m³ m⁻³)	θ_s (m³ m⁻³)	α (m⁻¹)	n (-)	K_s (m d⁻¹)
0 - 0.7	0.012	0.408	4.1	2.06	3.84
0.7 - 1.0	0.076	0.381	3.6	1.86	0.41
1.0 -1.5	0.032	0.403	6.4	2.26	3.41

215   Table 2 The RMSEs of simulated liquid water content obtained with different parameters

Parameters	10 cm	20 cm	30 cm	50 cm	70cm
Calibrated parameters	0.0213	0.0205	0.0289	0.0175	0.0231
Initial parameters	0.0485	0.0512	0.0553	0.0432	0.0427

3 Results and discussion

3.1 Field data showing freezing-induced water migration and water level decline

During the freezing stage from 28 NOV 2015 to 29 FEB 2016, there is a general trend of deepening frost depth (Fig. 1). The dates of the start of freezing, i.e., when soil temperature drops to 0 ℃, at 10 cm, 20 cm, 30 cm, 50 cm, and 70 cm are 02 DEC, 15 DEC, 16 DEC, 9 JAN and 23 JAN, respectively (Fig. 4). At 10 cm, 20 cm and 30 cm below surface, there is a sharp decrease in liquid water content when the soil temperature drops to 0 ℃, while at 50 cm and 70 cm below surface, due to freezing-induced water migration toward the freezing front, there is a gradual decrease in liquid water content before reaching a temperature of 0 ℃. At 90 cm below surface, probably because the freezing front is close enough to the sensor, although the temperature at the sensor does not reach 0 ℃, there is a significant decrease in liquid water content on 29 FEB due to freezing-induced water migration. Therefore, the relationship between temperature and liquid water content recorded by 5TM sensors, which are based on the frequency domain reflectometer (FDR) method, well reflects the effect of freezing on liquid water content.

Due to the rising air temperature in spring, soil temperature at 10 cm increased from below 0 ℃ to above 0 ℃ on 1 MAR, which is considered to be the start of the thawing stage in the current study. Because the water level is highest on 1 APR as a result of the downward infiltration of thawed water, 1 APR is considered to be the end of the thawing period. For the four sensors at 10 cm, 20 cm, 30 cm and 50 cm, the start dates of thawing

stage are 1 MAR, 2 MAR, 3 MAR, and 5 MAR, while for the sensor at 70 cm, the start date of thawing stage is 2

235   MAR, implying the occurrence of bi-directional thawing. Different from the quick response of soil temperature to

freezing, the response of soil temperature to thawing is a slow process. For the 3 sensors at 10 cm, 20 cm and 30

cm, the duration from start to end of thawing is 13 days, while for the 2 sensors at 50 cm and 70 cm, the durations

from start to end of thawing are 18 days and 26 days, respectively. The thawing of frozen soil is accompanied by

a trend of increasing liquid water content. The liquid water content at the end of thawing is much higher than that

before freezing, indicating the contribution of freezing-induced water gain.
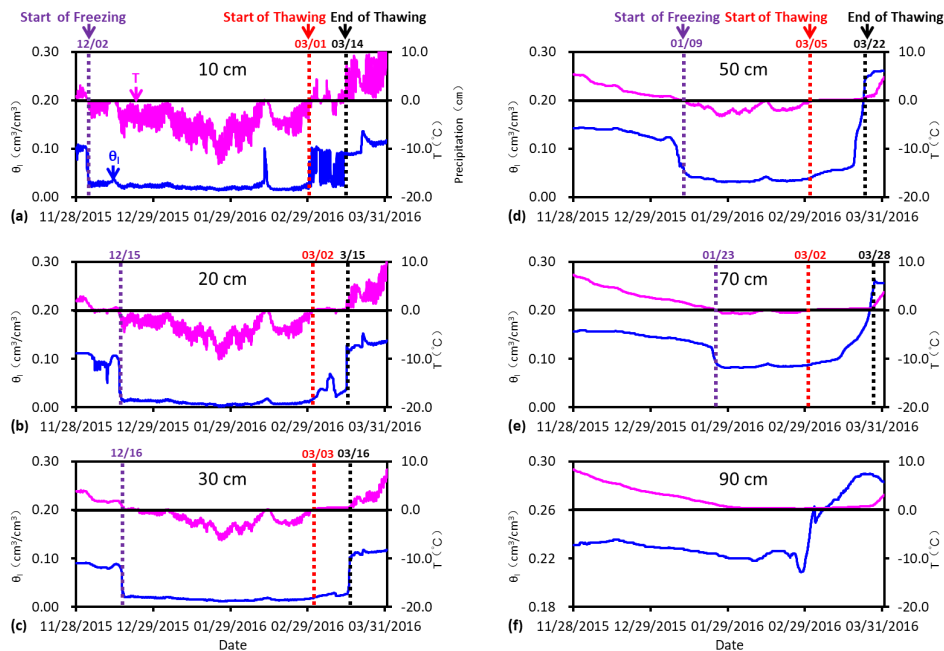
Figure 4 The observed hourly liquid water content and soil temperatures during the freezing-thawing cycle from

28 NOV 2015 to 1 APR 2016.

As shown in Fig. 1, water table depths on 28 NOV and 1 APR are 115 cm and 90 cm, respectively. Because

245   snowfall in winter is limited, the much higher water level at the end of thawing stage is mainly due to the

occurrence of lateral groundwater inflow as reported in Jiang et al. (2017). The lowest water level equaling 143

cm below surface occurs on 29 JAN. From 29 JAN, there is a trend of rising water level, which is one month

earlier than the occurrence of thawed water infiltration during the thawing stage. This phenomenon can also be

attributed to lateral groundwater inflow. The occurrence of lateral groundwater inflow also alleviated the

250   magnitude of freezing-induced groundwater level decline from 28 NOV to 29 JAN, i.e., freezing-induced

groundwater level decline should be greater than 28 cm. To quantify the water budget during the

freezing/thawing cycle, the abovementioned model is constructed to determine the fluxes of freezing-induced

migration, lateral groundwater flow, infiltration and soil evaporation.

3.2 Freezing-induced water redistribution: the effect of lateral groundwater flow and soil heterogeneity

255   Based on the parameters of van Genuchten (1980) and Mualem (1976) equation listed in Table 1, and the

lateral flow rate of 1.03 mm/d, there are good fits between simulated and measured liquid water content in the

frozen zone, and also for soil temperature (Fig. 5) and water level (Fig. 6a). Fig. 5 also shows the simulated total

water content, which coincides with liquid water content before freezing, but increases rapidly due to

freezing-induced water migration from the underlying soil and finally maintains at a stable value corresponding

260   to the completely frozen state. In the frozen zone, the magnitude of increase in total water content increases from

the shallow to the deep (Fig.5 and 6a), indicating that the distance to the water table not only controls the initial

liquid water content, but also the amount of freezing-induced water gain from underlying soils.
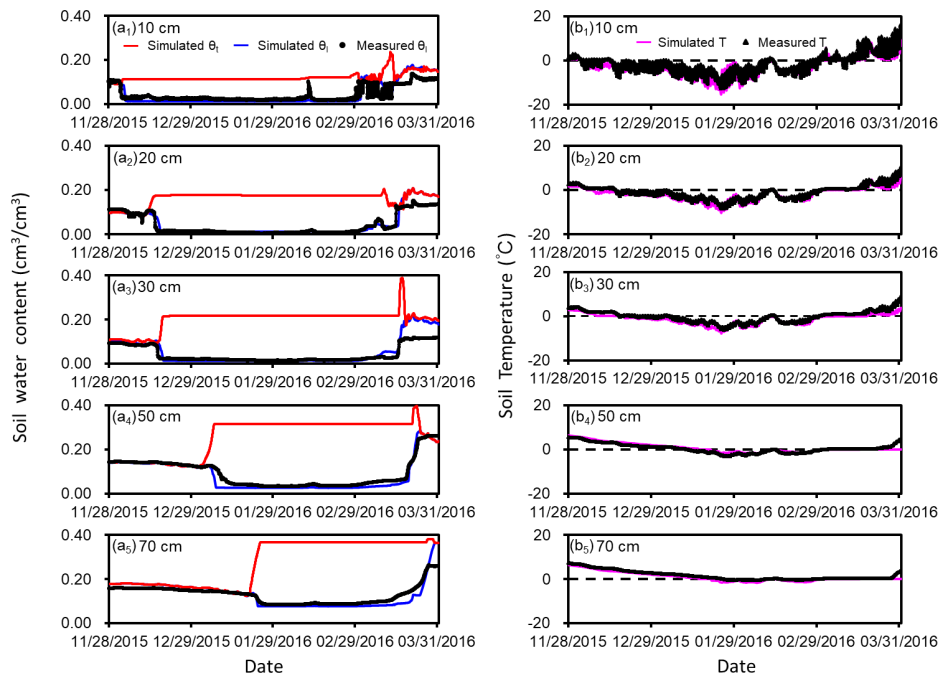
Figure 5   The observed and simulated liquid water content and simulated total water content (θ_t) (a_1-a_5) and soil

265   temperature (b_1-b_5) at the 5 different depths within the frozen zone during the freezing-thawing cycle.
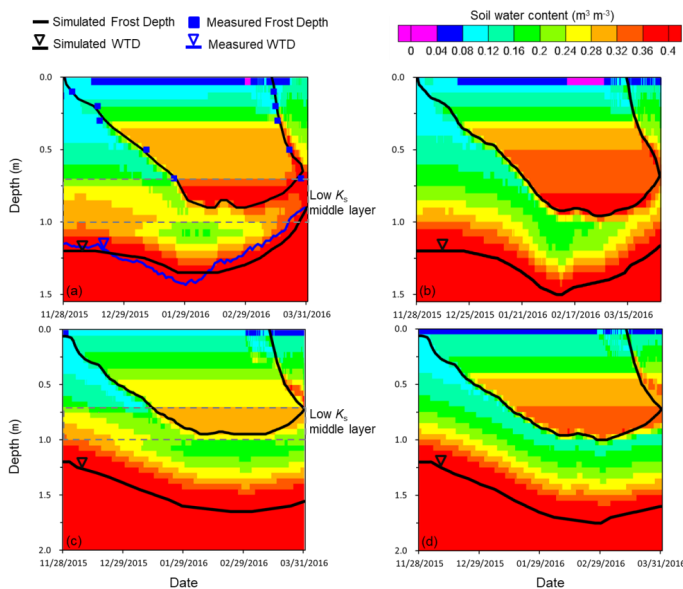
Figure 6 The frost depth, groundwater level and total water content under the four scenarios. (a) Scenario A, heterogeneous soil profile with a lateral flow rate of 1.03 mm/d; (b) Scenario B, homogeneous soil profile with a lateral flow rate of 1.03 mm/d; (c) Scenario C, heterogeneous soil profile without lateral inflow; (d) Scenario D,

270 homogeneous soil profile without lateral inflow.

Soil texture and the corresponding hydraulic conductivity are also factors controlling the flux of freezing-induced water migration through the unfrozen zone. Because the soil texture in the layer from 70 cm to 100 cm is slightly different from overlying and underlying soils, we compare the distribution of total water

275 content under the homogeneous case (Scenario B, Fig. 6b) with that of the base case (Scenario A, Fig. 6a). We find the low K_s of the middle layer restricts water migration into the part of frozen zone overlying the middle layer. As shown in Table 3, the increase of total water content in the frozen zone is 0.126 for Scenario B (corresponding to an increased water storage of 119.7 mm), and is 0.106 for Scenario A (corresponding to an increased water storage of 96.1 mm). Scenario A also has a smaller magnitude of freezing-induced water table

280 decline (Table 3). Moreover, due to the ability of clay to retain more water, before late January when the frost depth is still away from the middle layer, the middle layer shown in Fig. 6a has more liquid water than that shown in Fig. 6b; from late January to late February when the freezing front in Fig. 6a is shallower than the bottom of the middle layer, the unfrozen part of the middle layer also has higher water content than the underlying soil.

285   Table 3 A comparison of water table decline (ΔWTD), frost depth (FD), and water gain in the frozen zone under different groundwater conditions.

Groundwater conditions	Heterogeneous (low Ks middle layer)					Homogeneous				
	ΔWTD (mm)	FD (cm)	ΔS_{FZ} (mm)	ΔTWC	Mean TWC	ΔWTD (mm)	FD (cm)	ΔS_{FZ} (mm)	ΔTWC	Mean TWC
Fixed WTD=1.2 m	0	90	114.5	0.127	0.283	0	95	142.8	0.150	0.304
LFR=1.03 mm/d	15	90	96.1	0.106	0.265	30	95	119.7	0.126	0.282
LFR=0 mm/d	40	95	67.3	0.071	0.236	55	100	94.1	0.094	0.256

ΔS_{FZ} represents increased water storage in the frozen zone, ΔTWC represents increased total water content in the frozen zone, and Mean TWC represents the mean total water content in the frozen zone at the state of completely frozen.

290   Lateral groundwater flow is a component of water budget influencing water level. When there is no lateral groundwater flow, in either the heterogeneous case (Scenario C, Fig. 6c) or the homogeneous case (Scenario D, Fig. 6d), the lowest water level occurs at the end of the freezing stage. By comparing the simulated groundwater level under a series of lateral groundwater inflow rates, we find the occurrence of lateral groundwater inflow alleviates the magnitude of freezing-induced water level decline, and leads to a trend of earlier water level rise

295 before the start of the thawing stage (Fig. 7). Therefore, in the field, the existence of lateral groundwater inflow can be determined by the earlier occurrence of groundwater level rise before the start of the thawing stage. Due to the occurrence of lateral groundwater inflow, the rise in water level from late January to late February also restricts the frost depth to some extent (Table 3).
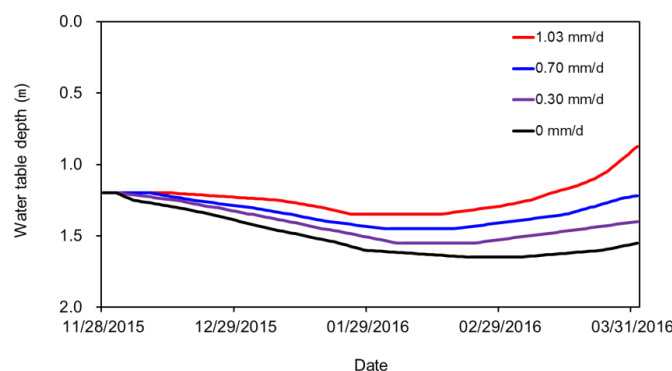
300   Figure 7 The temporal variations of simulated water table depth under different lateral groundwater inflow rates.

The higher water level caused by lateral groundwater flow would be beneficial for freezing-induced water migration towards the freezing front. In the heterogeneous cases, the increase in total water content in the frozen zone is found to be 0.106 in Scenario A, but is only 0.071 in Scenario C without lateral groundwater flow; in the homogeneous cases, the increase in total water content in the frozen zone is found to be 0.126 in Scenario B, but

305 is only 0.094 in Scenario D without lateral groundwater flow (Table 3). Therefore, compared with scenarios without lateral groundwater inflow, the occurrence of lateral groundwater inflow can inevitably lead to an increased freezing-induced water accumulation.

If a fixed head equaling 1.2 m below surface is assigned at the lower boundary, the increase in total water content in the frozen zone is 0.127 for the heterogeneous case, and is 0.150 for the homogeneous case (Table 3).

310 This confirms that a fixed head lower boundary condition would inevitably overestimate freezing-induced water migration. As we pointed out in the Introduction part, a fixed head lower boundary condition implies instantaneously replenishment of groundwater. The results shown in Fig. 7 indicate that an even larger groundwater inflow is needed to maintain a stable water level.

3.3 Soil evaporation during the freezing-thawing cycle

315 By comparing model results with and without consideration of the three snowfall events, we find snowfall did not infiltrate into the soil column due to the low permeability of frozen soil and got evaporated directly, implying that soil water evaporation is the only form of water loss leaving the top of the soil column during the freezing-thawing cycle. Therefore, we use the evaporation rate without considering snowfall events to represent actual soil evaporation. Note that although snowfall is not considered, the atmospheric conditions associated with

320 the snowfall event on 13 FEB still result in higher evaporation rate (Fig. 8).

Based on the trend of evaporation rate versus time, we identify three stages of soil water evaporation. Stage Ⅰ has a trend of decreasing evaporation rate, stage Ⅱ has a limited evaporation rate, and stage Ⅲ has a trend of increasing evaporation rate. In both scenarios, the start of stage Ⅱ corresponds to a frost depth of around 20 cm. In Scenario A, the mean evaporation rates in the three stages are 0.36, 0.18 and 0.59 mm/d, respectively (Fig. 8a),

325 leading to a cumulative evaporation of 32.1 mm; in Scenario B, the mean evaporation rates in the three stages are 0.53, 0.21 and 1.55 mm/d (Fig. 8b), respectively, corresponding to a cumulative evaporation of 55.3 mm. The high evaporation rate in stage Ⅲ, which is a direct result of accumulation of liquid water during the thawing stage, well explains the occurrence of soil salinization in spring (Liu et al., 2009;Lopez et al., 2010;Bechtold et al., 2011). Similar three stages of temporal evolution of soil evaporation during the freezing-thawing cycle have

330   been reported in several field studies (Kaneko et al., 2006;Wu et al., 2016;Xue et al., 2020).
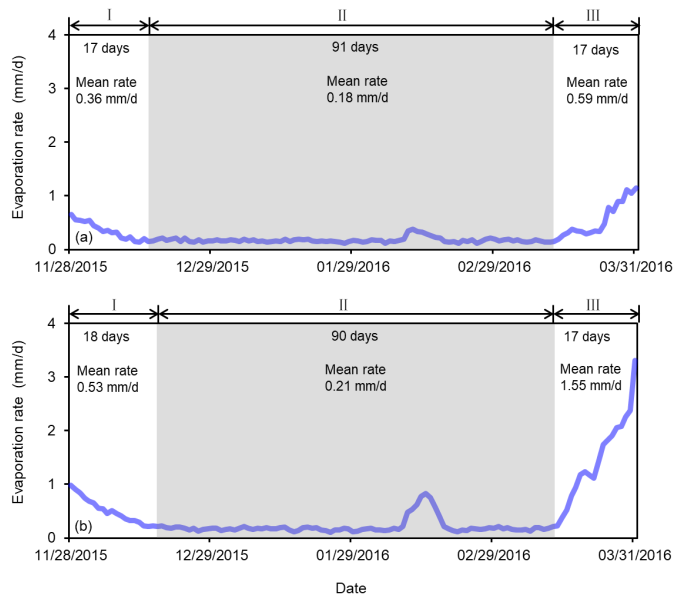
Figure 8 The simulated daily soil evaporation for Scenario A (a) and Scenario B (b). Also shown is the mean
evaporation rate for each stage.

335   In subsect. 3.2, based on the difference of total water content between the beginning and the end of the
freezing stage, the increased water storage in the frozen zone induced by freezing was calculated to be 96.1 mm
for Scenario A, and 119.7 mm for Scenario B. Considering the amount of water loss leaving the soil column due
to soil evaporation, the actual cumulative freezing-induced water migration into the frozen zone should be 115.6
mm for Scenario A and 146.0 mm for Scenario B. Therefore, a clear quantification of soil evaporation is critical
340   to understanding interactions of soil water and groundwater induced by freezing.

3.4 Water budgets during the freezing/thawing cycle

Because almost all snowfall are evaporated without entering the subsurface, soil evaporation and lateral
groundwater inflow are the only two processes influencing the balance of water in the soil column. If the
freezing/thawing cycle is divided into the freezing stage and the thawing stage, the balance of water in each stage
345   can be written as

$$S_{s0} + S_{u0} + q \cdot \Delta t_F = S_{s1} + S_{u1} + ET_F \cdot \Delta t_F \tag{6a}$$

$$S_{s1} + S_{u1} + q \cdot \Delta t_T = S_{s2} + S_{u2} + ET_T \cdot \Delta t_T \tag{6b}$$

where S_{s0} [L], S_{s1} [L] and S_{s2} [L] are cumulative water storages in the saturated zone at the beginning of freezing

stage, at the end of freezing stage (beginning of thawing stage) and at the end of the thawing stage, respectively;

350 S_{u0} [L], S_{u1} [L] and S_{u2} [L] are cumulative water storages in the unsaturated zone at the beginning of freezing stage,

at the end of freezing stage (beginning of thawing stage) and at the end of the thawing stage, respectively; q [L/T]

is the mean rate of lateral groundwater inflow during the freezing/thawing cycle; Δt_F [T] and Δt_T [T] are the

durations of the freezing and thawing stages, respectively; ET_F [L/T] and ET_T [L/T] are the mean soil

evaporation rates during the freezing and the thawing stages, respectively. The values of each term in Eq. (8) are

355 listed in Table 4.

Table 4 Water budgets during the freezing-thawing cycle

Stage	Duration	Δt	Initial S_s	Initial S_u	$q \cdot \Delta t$	$ET \cdot \Delta t$	Final S_s	Final S_u
		(d)	(mm)	(mm)	(mm)	(mm)	(mm)	(mm)
Freezing	28 NOV 2015 - 28 FEB 2016	93	120.9	246.4	95.8	19.5	80.6	362.9
Thawing	29 FEB 2016 - 1 APR 2016	32	80.6	362.9	33.0	12.6	239.6	224.4

Apparently, the groundwater loss during the freezing stage is calculated by $S_{s0} - S_{s1}$, which equals 40.3

mm and corresponds to a water table decline of 10 cm. In fact, such a water table decline has been alleviated by

360 the lateral groundwater inflow. The freezing-induced groundwater loss should be calculated by $S_{s0} - S_{s1} + q \cdot \Delta t_F$,

which equals 136.1 mm. In a groundwater flow model without considering the unsaturated zone, this process can

be characterized by a mean upward groundwater flux of 1.46 mm/d with a duration of 93 days at the upper

boundary. This is consistent with the dominance of upward flux at the upper boundary in the unfrozen period at

the study site (Jiang et al., 2017). Therefore, the current study confirms that shallow groundwater in the discharge

365 area of a semi-arid catchment is dominated by upward flow, which is consistent with the direction of regional

groundwater flow in the discharge area (Hubbert, 1940; Toth, 1962).

Similarly, in the thawing stage, groundwater gain from downward infiltration should be calculated by

$S_{s2} - S_{s1} - q \cdot \Delta t_T$, which equals 126.0 mm. In a groundwater flow model, this process can be characterized by a

mean downward groundwater flux of 3.94 mm/d at the upper boundary with a duration of 32 days. As

370 demonstrated in Jiang et al. (2017), in the unfrozen period, the stage from late SEP 2014 to early OCT 2014 (with

a duration of 18 days) is the only stage with net infiltration in our study site, and the net downward groundwater

flux equals 2.99 mm/d. The current study indicates that the thawing stage has an even larger downward

groundwater flux. Therefore, it is interesting to examine the pattern of two-dimensional or three-dimensional

groundwater flow induced by the freezing-thawing cycle by using a fully coupled soil-groundwater freeze-thaw

375   model in the future.

4 Conclusions

Based on field observations of soil temperature, liquid soil water content and groundwater level in the discharge area of a catchment, it was found that the observed temporal variations of wintertime liquid water content and groundwater level are not only controlled by freezing and thawing, but also by lateral groundwater

380   inflow. Therefore, a model is built to examine the responses of soil water and groundwater to wintertime climatic conditions and occurrence of lateral groundwater inflow in the saturated part of the soil column. The calibrated model increases our understanding of water balance as well as freezing-induced water migration during the freezing-thawing cycle.

Our model results showed that almost all snowfall is evaporated without infiltrating into the soil column due

385   to the low permeability of frozen soil. Therefore, soil evaporation is the only form of water loss, while lateral groundwater inflow is the only source of water gain. By comparing models with and without lateral groundwater inflow, we found the occurrence of lateral groundwater inflow led to much smaller magnitude of freezing-induced water level decline, and a trend of rising water level before the start of the thawing stage. Consequently, compared with the case without lateral groundwater inflow, the higher water level due to lateral

390   groundwater inflow resulted in much larger freezing-induced water migration into the frozen zone. We also found the middle layer with lower saturated hydraulic conductivity restricts both evaporation rates and freezing-induced water migration.

Based on the budget of groundwater during the freeing-thawing cycle, the mean flux of freezing-induced groundwater loss in the freezing stage with a duration of three months is 1.46 mm/d, and the mean flux of

395   thawing-induced groundwater gain in the thawing stage with a duration of one month is found to be 3.94 mm/d. As found by Jiang et al. (2017), due to the semi-arid climate, the only stage with net recharge in the unfrozen period is from late September to early October. Therefore, combined with the fluxes obtained by Jiang et al. (2017) for the unfrozen period, the fluxes during the freeing-thawing cycle obtained in the current study can be useful for future transient groundwater flow models to characterize the control of climatic conditions on

400   groundwater flow in semi-arid regions with seasonally freezing and thawing processes.

Code/Data availability

The numerical models in the current study were built by using the SHAW model (vision 3.0), which is available at https://www.ars.usda.gov/pacific-west-area/boise-id/watershed-management-research/docs/shaw-model/.

405   The meteorological data of the Otak station is available from China Meteorological Data Service Center (http://data.cma.cn).

The observed soil temperature, liquid water content and water table depth from 28 NOV 2015 to 1 APR 2016 at the field site are available in the supplement document.

410   **Author contribution**

XJ designed the field site and HX was involved in data collection. All authors were involved in data interpretation. XJ and LW developed the initial idea of the current study, and HX established the models with inputs from all coauthors. HX and XJ wrote the manuscript with contributions from YZ.

415   **Competing interests**

The authors declare that they have no conflict of interest.

Acknowledgements

This study is supported by the National Natural Science Foundation of China (41772242), the Fundamental

420   Research Funds for the Central Universities of China and the 111 Project (B20010).

References

Alkhaier, F., Flerchinger, G. N., and Su, Z.: Shallow groundwater effect on land surface temperature and surface energy balance under bare soil conditions: modeling and description, Hydrology and Earth System Sciences, 16, 10.5194/hess-16-1817-2012, 2012.

425   Bechtold, M., Haber-Pohlmeier, S., Vanderborght, J., Pohlmeier, A., Ferre, A., and Vereecken.H: Near-surface solute redistribution during evaporation, Geophysical Research Letters, 38, 17404, 10.1029/2011GL048147, 2011.

Bronfenbrener, L., and Bronfenbrener, R.: Frost heave and phase front instability in freezing soils, Cold Regions Science and Technology, 64, 19-38, 10.1016/j.coldregions.2010.07.001, 2010.

430   Carrera-Hernández, J. J., Smerdon, B. D., and Mendoza, C. A.: Estimating groundwater recharge through unsaturated flow modelling: Sensitivity to boundary conditions and vertical discretization, Journal of Hydrology, 452-453, 10.1016/j.jhydrol.2012.05.039, 2012.

Chamberlain, E. J.: Frost susceptibility of soil, review of index tests, Cold regoins research and engineering lab hanover NH, 1981.

435   Chen, J., Gao, X., Zheng, X., Miao, C., Zhang, Y., Du, Q., and Xu, Y.: Simulation of Soil Freezing and Thawing for Different Groundwater Table Depths, Vadose Zone Journal, 18:18057, 10.2136/vzj2018.08.0157, 2019.

Cherkauer, K. A., and Lettenmaier, D. P.: Hydrologic effects of frozen soils in the upper Mississippi River basin, Journal of Geophysical Research: Atmospheres, 104, 19599-19610, 10.1029/1999jd900337, 1999.

Daniel, J. A., and Staricka, J. A.: Frozen Soil Impact on Grounf Water‐Surface Water Interaction, JAWRA Journal
440   of the American Water Resources Association, 36, 151-160, 10.1111/j.1752-1688.2000.tb04256.x, 2000.

DeGaetano, A. T., Cameron, M. D., and Wilks, D. S.: Physical Simulation of Maximum Seasonal Soil Freezing Depth in the United States Using Routine Weather Observations, Journal of Applied Meteorology, 40, 546-555, 10.1175/1520-0450(2001)040<0546:psomss>2.0.co;2, 2001.

Demand, D., Selker, J. S., and Weiler, M.: Influences of Macropores on Infiltration into Seasonally Frozen Soil,
445   Vadose Zone Journal, 18, 10.2136/vzj2018.08.0147, 2019.

Dobinski, W.: Permafrost, Earth-Science Reviews, 108, 158-169, 10.1016/j.earscirev.2011.06.007, 2011.

Drescher, W. J.: Some effects of precipitation on ground water in Wisconsin, Wisconsin Geological Survey, 1955.

Evans, S. G., and Ge, S.: Contrasting hydrogeologic responses to warming in permafrost and seasonally frozen ground hillslopes, Geophysical Research Letters, 44, 1803-1813, 10.1002/2016gl072009, 2017.

450   Evans, S. G., Ge, S., Voss, C. I., and Molotch, N. P.: The role of frozen soil in groundwater discharge predictions for warming alpine watersheds, Water Resources Research, 54, 1599-1615, 10.1002/2017WR022098, 2018.

Fan, Y., Li, H., and Miguez-Macho, G.: Global patterns of groundwater table depth, Science, 339, 940-943, 10.1126/science.1229881, 2013.

Fetzer, Thomas, Vanderborght, Jan, Mosthaf, Klaus, Smits, Kathleen, M., Helmig, and Rainer: Heat and water

455   transport in soils and across the soil-atmosphere interface: 2. Numerical analysis, Water resources research, 53, 1080-1100, 10.1002/2016WR019983, 2017.

Flerchinger, G. N., and Saxton, K. E.: Simultaneous heat and water model of a freezing snow-residue-soil system I. Theory and development, Transactions of the ASAE, 32, 565-0571, 10.13031/2013.31040, 1989.

Flerchinger, G. N.: The simultaneous heat and water (SHAW) model: user's manual, Technical Rep. NWRC, 10,

460   2000.

Fuchs, M., Campbell, G., and Papendick, R.: An Analysis of Sensible and Latent Heat Flow in a Partially Frozen Unsaturated Soil 1, Soil Science Society of America Journal, 42, 379-385, 10.2136/sssaj1978.03615995004200030001x, 1978.

Gleeson, T., Marklund, L., Smith, L., and Manning, A. H.: Classifying the water table at regional to continental

465   scales, Geophysical Research Letters, 38, L05401, 10.1029/2010gl046427, 2011.

Hansson, K., and Lundin, L.-C.: Equifinality and sensitivity in freezing and thawing simulations of laboratory and in situ data, Cold Regions Science and Technology, 44, 20-37, 10.1016/j.coldregions.2005.06.004, 2006.

Harlan, R.: Analysis of coupled heat‐fluid transport in partially frozen soil, Water Resources Research, 9, 1314-1323, 10.1029/WR009i005p01314, 1973.

470   Hayhoe, H.: Field testing of simulated soil freezing and thawing by the SHAW model, Canadian Agricultural Engineering, 36, 279, 1994.

Hirota, T.: An extension of the force-restore method to estimating soil temperature at depth and evaluation for frozen soils under snow, Journal of Geophysical Research, 107, 4767, 10.1029/2001jd001280, 2002.

Hohmann, M.: Soil freezing — the concept of soil water potential. State of the art, Cold Regions Science &

475   Technology, 25, 101-110, 10.1016/S0165-232X(96)00019-5, 1997.

Hou, G., Liang, Y., Su, X., Zhao, Z., Tao, Z., Yin, L., Yang, Y., and Wang, X.: Groundwater Systems and Resources in the Ordos Basin, China, Acta Geologica Sinica, 82, 1061-1069, 10.1111/j.1755-6724.2008.tb00664.x, 2010.

Hubert, M.: The Theory of Ground-Water Motion, Soil Science, 51, 428, 10.1097/00010694-194105000-00015,

480   1940.

Ireson, A. M., van der Kamp, G., Ferguson, G., Nachshon, U., and Wheater, H. S.: Hydrogeological processes in seasonally frozen northern latitudes: understanding, gaps and challenges, Hydrogeology Journal, 21, 53-66, 10.1007/s10040-012-0916-5, 2013.

Iwata, Y., Hayashi, M., and Hirota, T.: Comparison of snowmelt infiltration under different soil-freezing conditions

485   influenced by snow cover, Vadose Zone Journal, 7, 79-86, 10.2136/vzj2007.0089, 2008.

Jiang, X.-W., Sun, Z.-C., Zhao, K.-Y., Shi, F.-S., Wan, L., Wang, X.-S., and Shi, Z.-M.: A method for simultaneous estimation of groundwater evapotranspiration and inflow rates in the discharge area using seasonal water table fluctuations, Journal of hydrology, 548, 498-507, 10.1016/j.jhydrol.2017.03.026, 2017.

Jiang, X. W., Wan, L., Wang, X. S., Wang, D., and Zhao, K. Y.: A multi-method study of regional groundwater

490   circulation in the Ordos Plateau, NW China, Hydrogeology Journal, 1657-1668, 10.1007/s10040-018-1731-4, 2018.

Kahimba, F. C., Ranjan, R. S., and Mann, D. D.: Modeling soil temperature, frost depth, and soil moisture redistribution in seasonally frozen agricultural soils, Applied engineering in agriculture, 25, 871-882, doi: 10.13031/2013.29237, 2009.

495   Kaneko, T., Kobayashi, T., Wang, W., and Cho, H.: Estimating Evaporation in Winter at a Field Irrigated Late in Autumn in Inner Mongolia, China, Journal Faculty of Agriculture Kyushu University, 51, 407-411, 10.1017/S0021859605005733, 2006.

Kurylyk, B. L., MacQuarrie, K. T., and Voss, C. I.: Climate change impacts on the temperature and magnitude of groundwater discharge from shallow, unconfined aquifers, Water Resources Research, 50, 3253-3274,

500   10.1002/2013WR014588, 2014.

Li, Q., Sun, S., and Xue, Y.: Analyses and development of a hierarchy of frozen soil models for cold region study, Journal of Geophysical Research Atmospheres, 115, 10.1029/2009JD012530, 2010.

Li, W., Brunner, P., Franssen, H. J. H., Li, Z., Wang, Z., Zhang, Z., and Wang, W.: Potential evaporation dynamics over saturated bare soil and an open water surface, Journal of Hydrology, 590, 125140,

505   10.1016/j.jhydrol.2020.125140., 2020.

Liu, Q., Cui, B., and Yang, Z.: Dynamics of the soil water and solute in the sodic saline soil in the Songnen Plain, China, Environmental Earth ences, 59, 837-845, 10.1007/s12665-009-0079-4, 2009.

Lopez, C. M. L., Brouchkov, A., Nakayama, H., Takakai, F., Fedorov, A. N., and Fukuda, M.: Epigenetic salt accumulation and water movement in the active layer of central Yakutia in eastern Siberia, Hydrological

510   Processes, 21, 103-109, 10.1002/hyp.6224, 2010.

Mualem, Y.: A new model for predicting the hydraulic conductivity of unsaturated porous media, Water resources research, 12, 513-522, 10.1029/WR012i003p00513, 1976.

Nelson, F. E.: (Un) frozen in time, Science, 299, 1673-1675, 10.1126/science.1081111, 2003.

Okkonen, J., Ala-Aho, P., Hänninen, P., Hayashi, M., Sutinen, R., and Liwata, P.: Multi-year simulation and model
515   calibration of soil moisture and temperature profiles in till soil, European Journal of Soil Science, 68, 829-839, 10.1111/ejss.12489, 2017.

Romano, N., Brunone, B., and Santini, A.: Numerical analysis of one-dimensional unsaturated flow in layered soils, Advances in Water Resources, 21, 315-324, 10.1016/S0309-1708(96)00059-0, 1998.

Rui, D., Zhai, J., Li, G., Zhang, J., and Suzuki, T.: Field experimental study of the characteristics of heat and water
520   transfer during frost heaving, Cold regions ence and technology, 168, 10.1016/j.coldregions.2019.102892, 2019.

Schneider, R.: Correlation of ground-water levels and air temperatures in the winter and spring in Minnesota: US Geol, Survey Water-Supply Paper, 1962, 1961.

Schuur, E. A. G., Mcguire, A. D., Sch?Del, C., ., Grosse, G., ., Harden, J. W., Hayes, D. J., Hugelius, G., ., Koven,
525   C. D., Kuhry, P., ., and Lawrence, D. M.: Climate change and the permafrost carbon feedback, Nature, 520, 171-179, 2015.

Shoop, S. A., and Bigl, S. R.: Moisture migration during freeze and thaw of unsaturated soils: modeling and large scale experiments, Cold Regions Science & Technology, 25, 33-45, 10.1016/S0165-232X(96)00015-8, 1997.

Stähli, M., Jansson, P.-E., and Lundin, L.-C.: Soil moisture redistribution and infiltration in frozen sandy soils,
530   Water Resources Research, 35, 95-103, 10.1029/1998wr900045, 1999.

Stephens, D.: Vadose zone hydrology, Lewis, Baca Raton, FL, 1996.

Tóth, J.: A theory of groundwater motion in small drainage basins in central Alberta, Canada, Journal of Geophysical Research, 67, 4375-4388, 10.1029/JZ067i011p04375, 1962.

Van Dam, J., and Feddes, R.: Numerical simulation of infiltration, evaporation and shallow groundwater levels
535   with the Richards equation, Journal of Hydrology, 233, 72-85, 10.1016/S0022-1694(00)00227-4, 2000.

van der Kamp, G.: The continuity between groundwater and soil water   in the prairie setting Proceedings of the NHRC workshop, 1992, 105-110,

van der Kamp, G., Hayashi, M., and Gallén, D.: Comparing the hydrology of grassed and cultivated catchments in the semi-arid Canadian prairies, Hydrological Processes, 17, 559-575, 10.1002/hyp.1157, 2003.

540   van Genuchten, M. T.: A closed-form equation for predicting the hydraulic conductivity of unsaturated soils 1, Soil Science Society of America Journal, 44, 892-898, 10.2136/sssaj1980.03615995004400050002x, 1980.

Vanderborgh, J., Fetze, T., Mostha, K., Smit, K. M., and Helmi, R.: Heat and water transport in soils and across the soil-atmosphere interface: 1. Theory and different model concepts, Water Resources Research, 53, 1057-1079, 10.1002/2016WR019982, 2017.

545   Walvoord, M. A., and Kurylyk, B. L.: Hydrologic Impacts of Thawing Permafrost—A Review, Vadose Zone Journal, 15, 10.2136/vzj2016.01.0010, 2016.

Wang, J. Z., Jiang, X. W., Wan, L., Worman, A., Wang, H., Wang, X. S., and Li, H.: An analytical study on artesian flow conditions in unconfined‐aquifer drainage basins, Water Resources Research, 51, 8658-8667, 10.1002/2015WR017104, 2015.

550   Wexler, A., Hyland, R., and Stewart, R.: Thermodynamic properties of dry air, moist air and water and SI psychrometric charts, ASHRAE, 1983.

Williams, P., and Smith, M.: The frozen earth: fundamentals of geocryology, Cambridge University Press, 1989.

Willis, W. O., Parkinson, H. L., Carlson, C. W., and Haas, H. J.: Water table changes and soil moisture loss under frozen conditions, Soil science, 98, 244-248, 10.1097/00010694-196410000-00005, 1964.

555   Wu, M., Huang, J., Wu, J., Tan, X., and Jansson, P.-E.: Experimental study on evaporation from seasonally frozen soils under various water, solute and groundwater conditions in Inner Mongolia, China, Journal of Hydrology, 535, 46-53, 10.1016/j.jhydrol.2016.01.050, 2016.

Xue, J., Feng, H., Chen, J., Zheng, X., and Du, Q.: The Effect of a Sand Interlayer on Soil Evaporation during the Seasonal Freeze–Thaw Period in the Middle Reaches of the Yellow River, Water, 12, 2092,
560   10.3390/w12082092, 2020.

Yorukoglu, M., and Celik, A. N.: A critical review on the estimation of daily global solar radiation from sunshine duration, Energy Conversion & Management, 47, 2441-2450, 10.1016/j.enconman.2005.11.002, 2006.

Yu, L., Zeng, Y., Wen, J., and Su, Z.: Liquid‐Vapor‐Air Flow in the Frozen Soil, Journal of Geophysical Research: Atmospheres, 123, 7393-7415, info:doi/10.1029/2018JD028502, 2018.

565   Yu, L., Zeng, Y., and Su, Z.: Understanding the mass, momentum, and energy transfer in the frozen soil with three levels of model complexities, Hydrology and Earth System Sciences, 24, 4813-4830, 10.5194/hess-24-4813-2020, 2020.

Zhang, T., Barry, R., Knowles, K., Ling, F., and Armstrong, R.: Distribution of seasonally and perennially frozen ground in the Northern Hemisphere, Proceedings of the 8th International Conference on Permafrost, 2003,

570   1289-1294,

Zhang, Y., Cheng, G., Li, X., Jin, H., Yang, D., Flerchinger, G. N., Chang, X., Bense, V. F., Han, X., and Liang, J.:
        Influences of Frozen Ground and Climate Change on Hydrological Processes in an Alpine Watershed: A Case
        Study in the Upstream Area of the Hei'he River, Northwest China, Permafrost and Periglacial Processes, 28,
        420-432, 10.1002/ppp.1928, 2017.

575   Zhang, Z., Wang, W., Gong, C., Wang, Z., Duan, L., Yeh, T. c. J., and Yu, P.: Evaporation from seasonally frozen
        bare and vegetated ground at various groundwater table depths in the Ordos Basin, Northwest China,
        Hydrological Processes, 10.1002/hyp.13404, 2019.

Zhang, Z., Li, Y., Barlage, M., Chen, F., and Li, Z.: Modeling groundwater responses to climate change in the
        Prairie Pothole Region, Hydrology and Earth System Sciences, 655-672, 10.5194/hess-2019-155, 2020.

580   Zhao, K. Y., Jiang, X. W., Wang, X. S., and Wan, L.: Restriction of groundwater recharge and evapotranspiration
        due to a fluctuating water table: a study in the Ordos Plateau, China, Hydrogeology Journal, 2, 1-11,
        10.1007/s10040-020-02208-9, 2020.

Zhu, Y., Ren, L., Skaggs, T. H., Lue, H., Yu, Z., Wu, Y., and Fang, X.: Simulation of Populus euphratica root uptake
        of groundwater in an arid woodland of the Ejina Basin, China, Hydrological Processes, 23, 2460-2469,
585   10.1002/hyp.7353, 2010.